Anal. Chem. **2008,** *80,* 3593–3597

Bioassembled Nanocircuits of $Mo_6S_{9-x}I_x$ Nanowires for Electrochemical Immunodetection of Estrone Hapten

Nijuan Sun,[†] Martin McMullan,[‡] Pagona Papakonstantinou,*[,‡] Hui Gao,[†] Xinxiang Zhang,[†] Dragan Mihailovic,[§] and Meixian Li*[,†]

College of Chemistry and Molecular Engineering, Peking University, Beijing, 100871, People's Republic of China, Nanotechnology and Integrated Bioengineering Centre, University of Ulster, Newtownabbey, County Antrim BT37 0QB, Northern Ireland, U.K., and Jozef Stefan Institute, Jamova 39, SI-1000 Ljubljana, Slovenia

We demonstrate a novel and highly sensitive electrochemical detection of estrone based on an immunosensor platform, composed of bioassembled nanocircuits of $Mo_6S_{9-x}I_x$ nanowires (MoSI NWs) covalently connected to anti-estrone antibodies. The one-step, label-free, and quantitative detection of estrone is realized by employing the $[Ru(NH_3)_6]^{3+/2+}$ redox ions to sense anti-estrone antibody and estrone interactions. The MoSI NWs/anti-estrone antibody nanocircuit architectures provide an amplification and conductive pathway for the specific electrochemical sensing of estrone hapten. A detection limit of 1.4 pg·mL^{-1} was achieved in contrast to previous electrochemical techniques in which the sensitivity was limited to the nanomolar range.

Naturally occurring estrogens, including estradiol and its most common metabolites and/or precursors (estrone (E1) and/or estriol), play a very important role in women's fertility. Changes in the concentration of estrogens are closely linked to human's health status,[1] and as a result their detection has gained significant attention. In the past, the most widely used methods for analyzing estrogens are chromatographic techniques such as gas chromatography (GC) or high-performance liquid chromatography (HPLC), but their sensitivity and selectivity limited their direct use for determination of these contaminants at a very low concentration level in environmental samples with a complex matrix. Recent developments have produced coupled techniques for specific detection of estrogens;[2–11] where the limit of detection (LOD) was greatly enhanced. For example, for E1, the LODs of GC-MS[3–5] have been reported to range from 0.02 to 0.4 ng·g^{-1}, 0.06−0.1 ng·g^{-1} for tandem GC-MS/MS,[6] 30−70 pg·L^{-1} for liquid chromatography-time of flight-mass spectrometry (LC-TOF-MS),[7] 20−60 pg·L^{-1} for LC-MS/MS,[8,9] and 0.25 ng·mL^{-1} for HPLC-UV.[10] The utilization of these developed coupled techniques provided a significantly lower limit of detection in the range of tens of picograms per liter. However, the high cost, complexity, large instrument size, and the application of organic reagents limit their further development and access for online detection. Therefore the development of an ultrasensitive, simple, and environmentally friendly method for detecting and quantifying estrogen species is essential for the early diagnosis of diseases. Electrochemical immunosensors, developed rapidly in recent years through the rapid growth of nanotechnologies, have shown a huge potential in estrogen analogue detection. However, only a handful of papers have reported the determination of estrogens by electrochemical methods because of the difficulty in obtaining their electrochemical responses on the bare electrodes.[1,12]

Within recent years, the integration of biomolecular recognition with nanoscale materials has produced hybrid systems with new functionalities and has led to the development of nanoscale circuitry linkages, nanobiosensors, and magnetic nanodevices.[13–18] Different nanocolloids with biospecific recognition have been used as the building blocks of new nanoscale superstructures. Elec-

* To whom correspondence should be addressed. Phone: +86-10-62757953 (M.L.); +44-29-90368932 (P.P). Fax: +86-10-62751708 (M.L.); +44-28-90366863. E-mail: lmwx@pku.edu.cn (M.L.); p.papakonstantinou@ulster.ac.uk (P.P.).

[†] Peking University.

[‡] University of Ulster.

[§] Jozef Stefan Institute.

(1) Hu, S. S.; Wu, K. B.; Yi, H. C.; Cui, D. F. *Anal. Chim. Acta* **2002**, *464*, 209–216.

(2) Xu, X.; Roman, J. M.; Veenstra, T. D.; Van Anda, J.; Ziegler, R. G.; Issaq, H. J. *Anal. Chem.* **2006**, *78*, 1553–1558.

(3) Quintana, J. B.; Carpinteiro, J.; Rodriguez, I.; Lorenzo, R. A.; Carro, A. M.; Cela, R. *J. Chromatogr., A* **2004**, *1024*, 177–185.

(4) Choi, M. H.; Kim, K. R.; Chung, B. C. *Analyst* **2000**, *125*, 711–714.

(5) Chen, J.; Lichwa, J.; Snehota, M.; Mohanty, S.; Ray, C. *Chromatographia* **2006**, *64*, 413–418.

(6) Ternes, T. A.; Andersen, H.; Gilberg, D.; Bonerz, M. *Anal. Chem.* **2002**, *74*, 3498–3504.

(7) Reddy, S.; Brownawell, B. J. *Environ. Toxicol. Chem.* **2005**, *24*, 1041–1047.

(8) Tai, S. S. C.; Welsh, M. J. *Anal. Chem.* **2005**, *77*, 6359–6363.

(9) Beck, I. C.; Bruhn, R.; Gandrass, J.; Ruck, W. *J. Chromatogr., A* **2005**, *1090*, 98–106.

(10) Wang, L.; Cai, Y. Q.; He, B.; Yuan, C. G.; Shen, D. Z.; Shao, J.; Jiang, G. B. *Talanta* **2006**, *70*, 47–51.

(11) Mitani, K.; Fujioka, A.; Kataoka, H. *J. Chromatogr., A* **2005**, *1081*, 218–224.

(12) Gao, H.; Lu, J. Y.; Cui, Y. R.; Zhang, X. X. *J. Electroanal. Chem.* **2006**, *592*, 88–94.

(13) Patolsky, F.; Zheng, G. F.; Lieber, C. M. *Nanomedicine* **2006**, *1*, 51–65.

(14) Chang, M. M. C.; Cuda, G.; Bunimovich, Y. L.; Gaspari, M.; Heath, J. R.; Hill, H. D.; Mirkin, C. A.; Nijdam, A. J.; Terracciano, R.; Thundat, T.; Ferrari, M. *Curr. Opin. Chem. Biol.* **2006**, *10*, 11–19.

(15) Asuri, P.; Bale, S. S.; Karajanagi, S. S.; Kane, R. S. *Curr. Opin. Chem. Biol.* **2006**, *17*, 562–568.

(16) Zheng, G. F.; Patolsky, F.; Cui, Y.; Wang, W. U.; Lieber, C. M. *Nat. Biotechnol.* **2005**, *23*, 1294–1301.

(17) Lee, K. B.; Park, S.; Mirkin, C. A. *Angew. Chem., Int. Ed.* **2004**, *43*, 3048–3050. *Angew. Chem.* **2004**, *116*, 3110−3112.

(18) Yan, H.; Park, S. H.; Finkelstein, G.; Reif, J. H.; LaBean, T. H. *Science* **2003**, *301*, 1882–1884.

10.1021/ac7024893 CCC: $40.75
Published on Web 04/12/2008

tronic nanowire devices gain more and more attention since they can readily be integrated into miniaturized systems to enable detection and sensing through electrical readout.[19–22] Molybdenum−chalcogenide−halide nanowires (NWs), composed of molybdenum (Mo), sulfur (S), and iodine (I) in the form of $Mo_6S_{9-x}I_x$ (MoSI) are in particular a new class of quasi-one-dimensional objects.[23,24] Their potential to become unique building elements in biosensing devices has barely been noticed so far, in complete contrast to carbon nanotubes. MoSI NWs might offer opportunities to nicely complement carbon nanotubes in the detection of biomolecules by avoiding some of their drawbacks.[25,26] MoSI NWs are easily separable and have the tendency to monodisperse, with all nanowires having identical metallic, electronic properties. Most significantly they can act as molecular-scale connectors to bind thiolated proteins, providing an approach to the assembly of nanocircuits. Mihailovic et al. reported recently that the S atoms at the ends of MoSI NWs are capable of forming covalent bonds with a gold surface or with thiol groups of large molecules.[27]

Here, we describe for the first time a novel highly sensitive electrochemical detection of estrone based on an immunosensor from bioassembled nanocircuits of MoSI NWs. A one-step, specific, label-free, and quantitative detection of estrone is realized by monitoring the electrochemical responses of redox probe $[Ru(NH_3)_6]^{3+/2+}$ on the bioassembled nanocircuits resulting from association of estrone to MoSI NWs/anti-estrone antibody superstructures.

EXPERIMENTAL SECTION

Chemicals and Materials. Estrone (E1) and bovine serum albumin (BSA) were purchased from Sigma. Monoclonal anti-estrone antibody was prepared and purified from serum collected from the immunized mouse (Monoclonal Laboratories, Department of Biology, Peking University, China). Hexaammineruthenium(II) chloride [$Ru(NH_3)_6Cl_2$, 99.9+%] and hexaammineruthenium(III) chloride [$Ru(NH_3)_6Cl_3$, 98%] were purchased from Aldrich. Immunoreagents were dissolved in pH 7.2 phosphate-buffered saline (PBS) solution (0.01 M phosphate, 136 mM NaCl, 2.7 mM KCl) unless otherwise noted. Doubly distilled water was further purified with a quartz apparatus. Aqueous solutions were prepared with triply distilled water. Glass carbon electrodes were purchased from Lanlike Instrument Co. (Tianjing, China).

$Mo_6S_xI_{9-x}$ nanowires were fabricated by direct synthesis from elemental material that had been mixed in the desired stoichiometries, as described elsewhere.[22] Powders composed of aggregates of individual nanowires were obtained with two different stoichiometries $Mo_6S_3I_6$ and $Mo_6S_{4.5}I_{4.5}$. The stoichiometries were determined by a combination of techniques such as chemical analysis, high-resolution transmission electron microscopy, and X-ray photoelectron spectroscopy, as reported in the literature.[28] In this work, all studies were carried out on $Mo_6S_3I_6$ nanowires.

Preparation of $[Ru(NH_3)_6]^{2+/3+}$ redox probe solution was as follows: The $Ru(NH_3)_6Cl_2/Ru(NH_3)_6Cl_3$ (1:1, 1 mM) mixture was dissolved in PBS (10 mM, pH 7.2) solution, and 0.1 M KCl was added as the supporting electrolyte.

Fabrication of MoSI NWs Immunosensors. In 2-propanol, 1 mg·mL^{-1} MoSI dispersions were made. The dispersions were initially sonicated for 2 min using a high-power ultrasonic tip (120 W, 60 kHz) followed by a mild sonication for 2 h using a low-power ultrasonic bath. Prior to use, the dispersions were resonicated for 20 min to obtain uniform suspension, which was denoted as MoSI NWs suspension.

A glassy carbon electrode (GCE) was first polished with a 0.05 μm alumina slurry and then washed ultrasonically in triply distilled water and ethanol for a few minutes, respectively. Finally, the GCE was coated by casting 60 μL of MoSI NWs suspension and dried under an infrared lamp. This modified electrode is denoted as NWs/GCE.

Optimization of Immunoassay Conditions. A number of important factors for imparting an efficient signal transduction property on the NW immunosensor platform were investigated. These include the concentration of modified anti-estrone antibody, BSA blocking, antigen incubation time, temperature, and pH value of the PBS solution. The concentration of anti-estrone antibody was varied from 0.020 to 0.50 mg·mL^{-1}, where the electrochemical responses (peak currents of cyclic voltammetry (CV) and differential pulse voltammetry (DPV) in PBS solution containing $[Ru(NH_3)_6]^{2+/3+}$) of anti-estrone antibody modified NWs/GCE electrode (denoted as Ab-NWs/GCE) were saturated at concentrations above 0.066 mg·mL^{-1}. The Ab-NWs/GCE requires incubation in BSA to block nonspecific binding sites or else the typical sigmoid curve of immunoassay could not be obtained. An optimized incubation time of 4 h at 25 °C was established. Furthermore the effect of temperature on the immunoreaction was also investigated in the range of 20−45 °C. The maximum current response occurred at an incubation temperature of 32 °C when the Ab-NWs/GCE was incubated in 5 pg·mL^{-1} estrone; at the same time, with increasing incubation time, the electrochemical responses of the immunosensor increased and then reached a constant value when the incubation time was longer than 40 min. In addition, the appropriate pH range was optimized between 7.2 and 7.6. Briefly speaking, the optimal conditions for attachment of anti-estrone antibody to the NWs/GCE were incubation in 0.066 mg·mL^{-1} antibody (in 10 mM PBS, pH 7.2) for 12 h at 4 °C. After a careful rinse, the Ab-NWs/GCE was immediately incubated for 4 h at 25 °C with 0.2 mL of 1% BSA for blocking nonspecific

(19) Wang, W. U.; Chen, C.; Lin, K. H.; Fang, Y.; Lieber, C. M. *Proc. Natl. Acad. Sci. U.S.A.* **2005**, *102*, 3208–3212.

(20) Nishinaka, T.; Takano, A.; Doi, Y.; Hashimoto, M.; Nakamura, A.; Matsushita, Y.; Kumaki, J.; Yashima, E. *J. Am. Chem. Soc.* **2005**, *127*, 8120–8125.

(21) Herland, A.; Bjork, P.; Nilsson, K. P. R.; Olsson, J. D. M.; Asberg, P.; Konradsson, P.; Hammarstrom, P.; Inganas, O. *Adv. Mater.* **2005**, *17*, 1466–1471.

(22) Cui, Y.; Wei, Q. Q.; Park, H. K.; Lieber, C. M. *Science* **2001**, *293*, 1289–1292.

(23) Vrbanic, D.; Remskar, M.; Jesih, A.; Mrzel, A.; Umek, P.; Ponikvar, M.; Jancar, B.; Meden, A.; Novosel, B.; Pejovnik, S.; Venturini, P.; Coleman, J. C.; Mihailovic, D. *Nanotechnology* **2004**, *15*, 635–638.

(24) Mrzel, A.; Kova, J.; Remkar, M.; Jesih, A.; Mihailovi, D. *Synth. Met.* **2005**, *153*, 309–312.

(25) Nicolosi, V.; Vrbanic, D.; Mrzel, A.; McCauley, J.; O'Flaherty, S.; McGuinness, C.; Compagnini, G.; Mihailovic, D.; Blau, W. J.; Coleman, J. N. *J. Phys. Chem. B* **2005**, *109*, 7124–7133.

(26) Vrbanic, D.; Pejovnik, S.; Mihailovic, D.; Kutnjak, Z. *J. Eur. Ceram. Soc.* **2007**, *27*, 975–977.

(27) Ploscaru, M. I.; Kokalj, S. J.; Uplaznik, M.; Vengust, D.; Turk, D.; Mrzel, A.; Mihailovic, D. *Nano Lett.* **2007**, *7*, 1445–1448.

(28) Nicolosi, V.; Nellist, P. D.; Sanvito, S.; Cosgriff, E. C.; Krishnamurthy, S.; Blau, W. J.; Green, M. L. H.; Vengust, D.; Dvorsek, D.; Mihailovic, D.; Compagnini, G.; Sloan, J.; Stolojan, V.; Carey, J. D.; Pennycook, S. J.; Coleman, J. N. *Adv. Mater.* **2007**, *19*, 543–547.

Scheme 1. (A) Schematic Diagram of the Preparation of an Immunosensor: (a) Bare Electrode; (b) Electrode a Modified with 50 μL of MoSI NWs; (c) NWs/GCE Incubated in 0.066 mg·mL^{-1} Anti-estrone Antibody for 12 h for Immobilization of the Antibody on the Surface; (d) c Incubated in BSA for Blocking Nonspecific Adsorption. (B) Schematic View of Electrochemical Detection of Hapten Estrone by This Immunosensor

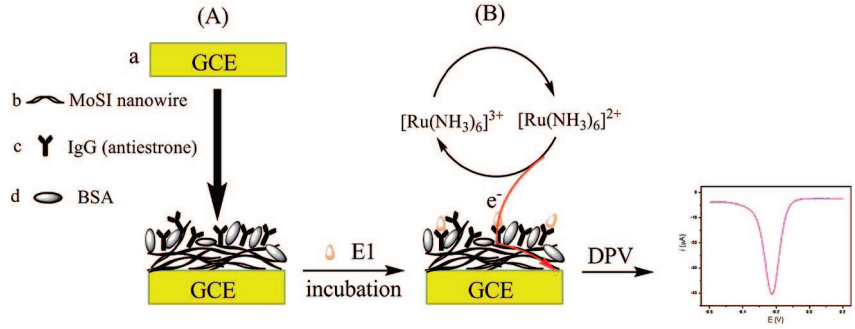

binding. All resulting electrodes were washed with PBS buffer and stored at 4 °C.

Immunosensing Detection of Estrone. Cyclic voltammetry and differential pulse voltammetry were performed in 10 mM PBS buffer (pH 7.2), containing 0.1 M KCl and 1 mM $Ru(NH_3)_6Cl_2$/$Ru(NH_3)_6Cl_3$ (1:1 mixture as a redox probe). For the CV measurement, the scan rate was 100 mV·s^{-1}, and the potential range was from +0.2 to −0.6 V. The DPV experiments were carried out in the same potential range as CV at a scan rate of 20 mV·s^{-1}; the pulse amplitude and the pulse width adopted were 50 mV and 60 ms, respectively. Before each measurement, the Ab-NWs/GCE was incubated in 2 mL of PBS buffer containing different concentrations of estrone at 32 °C for 40 min. It should be noted that the electrode in all steps was rinsed carefully with PBS solution and all the electrochemical experiments were carried out under nitrogen atmosphere.

Instrumentation. A CHI 660A electrochemical workstation (CH Instruments) was used for cyclic voltammetry and DPV at ambient temperature (20 ± 2 °C) in a three-electrode cell. The working electrode was a glassy carbon electrode with a diameter of 4 mm. A KCl saturated calomel electrode was used as the reference electrode, and a platinum foil with large surface area as the auxiliary electrode, respectively.

Atomic force microscopy (AFM) characterizations were performed in the tapping mode in air with a Nanoscope IIIa microscope (Digital Instruments). The samples were prepared as follows: 50 μL of supernatant liquor of MoSI NWs dispersion was dropped on the gold sheet and dried in air, and subsequently it was dipped in 10 mM PBS (pH 7.2) containing 0.2 mg·mL^{-1} IgG for 12 h (4 °C). The same electrochemical experiments were performed on both gold and glassy carbon electrodes, and similar results were obtained. AFM characterization was performed on gold substrate because the surface is much glossier and allowed one to observe the connection between MoSI NWs and IgG clearly.

RESULTS AND DISCUSSION

Before bioassembly, MoSI NWs were ultrasonicated in 2-propanol as described elsewhere[25,27] to produce a 1 mg·mL^{-1} dispersion with average bundle diameters of about 10−50 nm. Scheme 1 illustrates the construction process of the MoSI NWs immunosensor. This involves (i) casting MoSI NWs suspension on a bare glassy carbon electrode (GCE), (ii) immobilization of anti-estrone antibody (IgG) containing thiol groups by direct covalent connection to MoSI NWs, and (iii) incubation of the assembly in BSA to block nonspecific binding. This simple method is effective in retaining IgG activity after conjugation. The MoSI−IgG self-assembly was characterized by AFM. The MoSI−IgG bioconjugation is observed clearly in Figure 1A, which illustrates one terminal of a NW bundle attached to IgG. The IgG is attached to the end of the NWs through S−S bonding, as it was recently reported.[27] The corresponding height profiles in

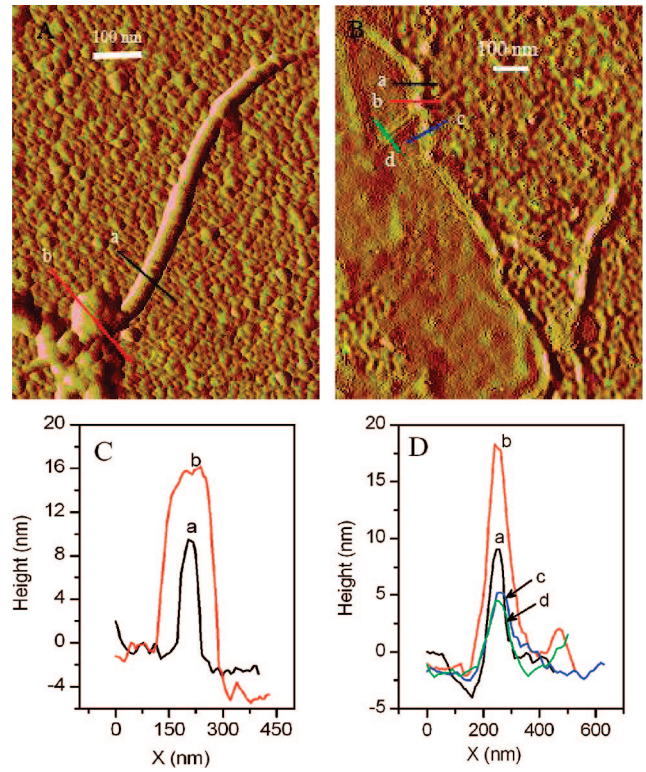

Figure 1. (A, B) AFM tapping mode images of the MoSI nanowires bundle attached to anti-estrone antibody with a S−S bond. Panel A illustrates one terminal of a NW bundle attached to IgG. Panel B shows multiterminal branches (positions a, d, and c) composed of junction points (position b) between bundles of NWs. The heights profiles (C, D) correspond to the positions which are marked by color coded letters in A and B, respectively.

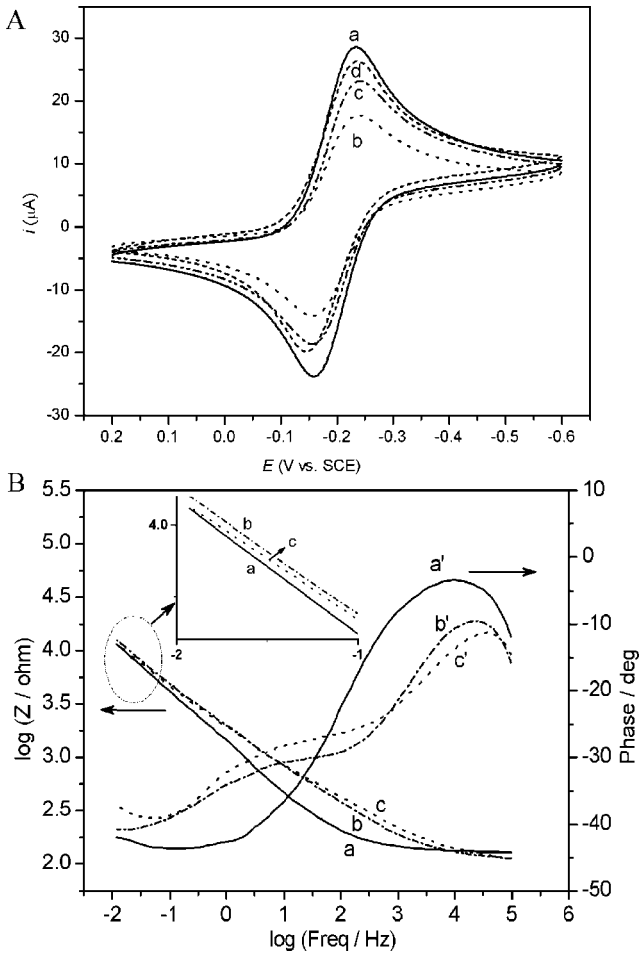

Figure 2. (A) Cyclic voltammograms of 1 mM $[Ru(NH_3)_6]^{3+/2+}$ redox probe characterizing each step of modification on the GCE at a scan rate of 100 mV·s^{-1}. (a) Bare GCE; (b) GCE in a modified with 50 μL of MoSI NWs; (c) immobilized anti-estrone antibody on b; (d) c incubated in BSA solution for blocking nonspecific adsorption. (B) Electrochemical impedance bode plots of bare GCE (a, a′), MoSI NWs modified GCE (b, b′), and IgG attached NWs modified GCE (c, c′). Inset in B is an amplified plot of the circle noting partialness in a low-frequency scale.

Figure 1C reveal an increase in diameter from 10 nm for the NW bundle to 16 nm for the MoSI−IgG aggregate. Multiterminal circuits composed of junction points between bundles of NWs were also formed as revealed in Figure 1B. The diameters of the three different branches were 9, 5.5, and 4.6 nm, respectively, whereas the diameter of the junction point of these three branches was 18 nm, which was regarded as composed MoSI−IgG aggregates (Figure 1D). The above images demonstrate that the MoSI NWs can act as nanoconnectors to allow the self-assembly of complex networks due to their chemical specificity with sulfur.

Each step of the fabrication of the bioassembled nanocircuits was characterized by cyclic voltammetry employing the redox couple of $[Ru(NH_3)_6]^{3+/2+}$ as probe ions (Figure 2A). Simultaneously, we investigated the coupling of the resulting interfaces by monitoring the electrical response as a function of frequency using electrochemical impedance spectroscopic measurements (EIS; Figure 2B). The cyclic voltammogram of the bare GCE showed one pair of well-defined, nearly reversible redox peaks at about −0.2 V (Figure 2A, curve a). Both reduction and oxidation peak currents decreased upon immobilization of the MoSI NWs

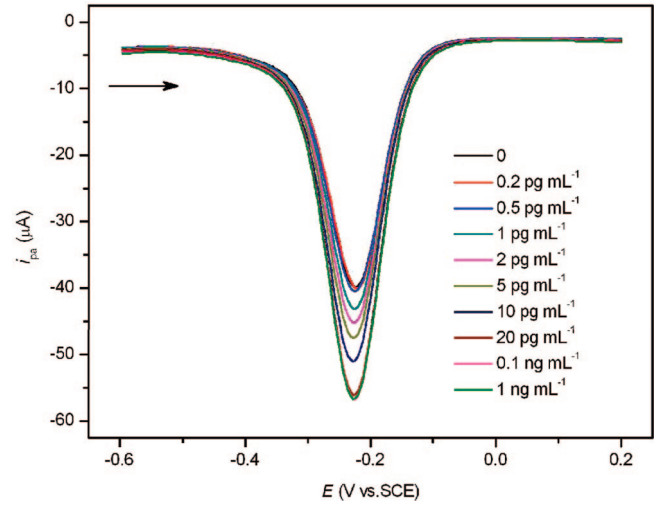

Figure 3. Differential pulse voltammograms of the Ab-NWs/GCE immunosensor incubated in different concentrations (from 0.2 pg·mL^{-1} to 1 ng·mL^{-1}) of estrone. Pulse amplitude and the pulse width adopted are 50 mV and 60 ms, respectively. The scan rate is 20 mV·s^{-1}.

(NWs/GCE; Figure 2A, curve b) due to the increase in the resistance of the ohmic contact between the NWs and the GCE. This was confirmed by the EIS response in the form of bode plot (Figure 2B), where the module of impedance in the low-frequency ranges increased slightly upon the association of the NWs to the GCE. Moreover the phase diagram showed an obvious difference from that of the bare electrode. Compared to the single-peak behavior for the bare electrode, the modified electrode was accompanied by two peaks indicating the nonideal communication between GCE and MoSI NWs. Connection of the anti-estrone antibody to the NWs via the formation of S−S covalent bonds between the S atoms of the NWs and the thiol groups of anti-estrone antibody molecules resulted in an increase of the redox peak currents (Figure 2A, curve c). This rise of the current is ascribed to attraction of anti-estrone antibody to the redox probe ion. Anti-estrone antibody (isoelectric point is 4.7−6.5) develops a negative surface charge in PBS buffer solution (pH 7.2), which attracts the positive probe ion and accelerates its interfacial electron-transfer rate. A decrease in the module of impedance illustrated in the inset of Figure 2B is consistent with the rise in the peak current. Further increase of the redox peak currents was observed upon immobilization of BSA for blocking any nonspecific adsorption on the electrode. The increase is attributed to the static interaction between BSA (isoelectric point is 4.7−4.8) and $[Ru(NH_3)_6]^{3+/2+}$ (Figure 2A, curve d). Upon the association of the MoSI−anti-estrone antibody−BSA conjugate to estrone, the electrochemical responses of the redox probe dramatically increased. The reason for this might be the formation of bioassembled nanocircuits, accelerating the electron transfer of the redox probe, as illustrated in the Scheme 1. On the basis of this, the sensitivity of the designed immunoassay was evaluated by conducting a series of experiments employing DPV in which the concentration of estrone varied from 2×10^{-13} to 1×10^{-9} g·mL^{-1}, as shown in Figure 3. With increasing concentrations of estrone, the current response of the modified electrode increased. A typical sigmoid curve presenting the peak current versus estrone concentration in logarithmic scale was obtained, as shown in

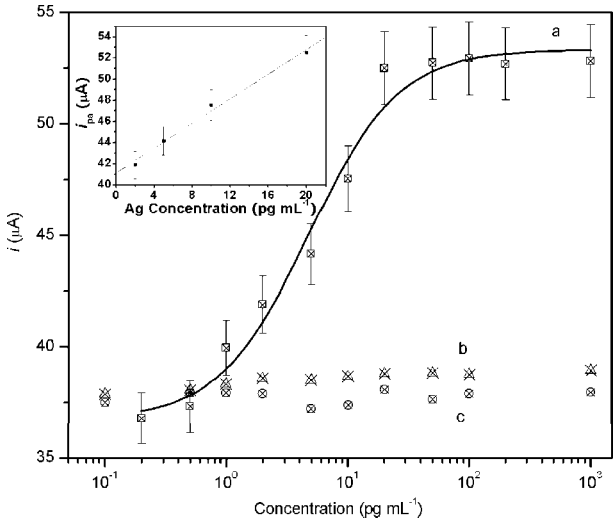

Figure 4. Calibration curves for the current responses of different concentrations of estrone on the Ab-NWs/GCE (a), NWs/GCE (b), and bare GCE (c). The inset shows a linear part of curve a.

Figure 4. Every point corresponds to the average value of three independent measurements. In it, the linear range was from 2×10^{-12} to 2×10^{-11} g·mL^{-1}, and the regression equation was i (μA) $= 41 + 0.58(C$ (pg·mL^{-1})) ($R = 0.995$). The detection limit was 1.4 pg·mL^{-1}, which compares favorably with those reported previously.[2–11] The relative standard deviation for the fixed concentration of 5×10^{-12} g·mL^{-1} estrone with ten-times replicative preparations of the immunosensor was found to be 4%. These results suggest that the immunosensor has high sensitivity and reproducibility.

To confirm that the electrochemical readout originates from the specific interaction between anti-estrone antibody and estrone hapten as well as to elucidate the role of the MoSI NWs, the following control experiments were performed: First, all the steps in the construction process were followed except for the incubation in anti-estrone antibody. The resulting current changes for different concentrations of estrone hapten were irregular and insignificant, as shown in curve c of Figure 4. This validates our assertion that sensing of estrone mainly is a consequence of a specific interaction, rather than the result of electrostatic interactions or other nonspecific interactions. Second, all the steps of the construction process were repeated on a bare GCE without the association of MoSI NWs. The produced signals were also unimportant (Figure 4, curve b), which indicates that the presence of MoSI NWs provides a significant amplification of the electrochemical signal. Both control experimental results suggest that the obvious current enhancement of the redox probe is attributed to the electrical wiring of the anti-estrone antibody to MoSI NWs as well as to the specific antibody and hapten bioconjugation resulting in the formation of bioassembled nanocircuits. The assembly of anti-estrone antibody−NWs superstructures with a fairly high level of complexity and organization acts as a powerful sensing matrix for estrone.

CONCLUSIONS

We have developed a novel immunosensor based on the relatively unexplored MoSI NWs and the specific interaction between anti-estrone antibody and estrone hapten. Our approach bridges the elements of molecular recognition and the unique features of nanowires to yield architectures with novel sensing functions. The high sensitivity of the MoSI NWs immunosensor is related to the following unique attributes: (a) the MoSI NWs provide a high density of sulfur ends and hence a high density of primary anti-estrone antibodies; (b) the highly conductive MoSI NWs act as molecular connectors to anti-estrone antibody and at the same time cause the formation of nanocircuit architectures, which provide a conductive pathway for the electrochemical sensing of estrone hapten. A detection limit of 1.4 pg·mL^{-1} was achieved in contrast to previous electrochemical techniques in which the sensitivity was limited to the nanomolar range. This bioassay could be applied to the detection of trace estrone produced by human or other animals. This is the first time to report the construction of bioassembled nanocircuits of MoSI NWs as a powerful diagnostic platform. The organization of superstructures consisting of MoSI NWs cross-linked with thiolated proteins, DNA, or semiconducting nanoparticles could yield new architectures for biosensing, fuel cells, and photonic applications or novel configurations for photoelectrochemical cells.

ACKNOWLEDGMENT

This work has been supported by Royal Society (U.K.−China Joint Project), the National Natural Science Foundation of China (Grants 20575004 and 20735001), and GlaxoSmithKline for providing a CAST studentship to M.M.

Received for review December 7, 2007. Accepted March 9, 2008.

AC7024893